© 2019. Published by The Company of Biologists Ltd | Journal of Experimental Biology (2019) 222, jeb193730. doi:10.1242/jeb.193730

SHORT COMMUNICATION

Visuomotor strategies for object approach and aversion in *Drosophila melanogaster*

Jean-Michel Mongeau*,‡, Karen Y. Cheng, Jacob Aptekar and Mark A. Frye

ABSTRACT

Animals classify stimuli to generate appropriate motor actions. In flight, *Drosophila melanogaster* classify equidistant large and small objects with categorically different behaviors: a tall object evokes approach whereas a small object elicits avoidance. We studied visuomotor behavior in rigidly and magnetically tethered *D. melanogaster* to reveal strategies that generate aversion to a small object. We discovered that small-object aversion in tethered flight is enabled by aversive saccades and smooth movement, which vary with the stimulus type. Aversive saccades in response to a short bar had different dynamics from approach saccades in response to a tall bar and the distribution of pre-saccade error angles was more stochastic for a short bar. Taken together, we show that aversive responses in *D. melanogaster* are driven in part by processes that elicit signed saccades with distinct dynamics and trigger mechanisms. Our work generates new hypotheses to study brain circuits that underlie classification of objects in *D. melanogaster*.

KEY WORDS: Behavioral algorithm, Flight, Fruit fly, Saccade, Smooth movement

INTRODUCTION

Animals on the move must rapidly integrate and evaluate sensory information to generate appropriate motor actions. For instance, flies must distinguish between potential threats, a landing site or a food source while locomoting through spatiotemporally complex environments (Frye and Dickinson, 2001). Often, a decision must be generated extremely quickly to avoid predation (Muijres et al., 2014), leaving little time for sensorimotor processing (Mongeau et al., 2015). A compelling hypothesis for rapid decision making is that feature-selective neurons relay salient information to trigger appropriate behavior (Sen et al., 2017; Wu et al., 2016). For instance, a looming object generates stereotyped expanding optic flow that can be passed on to appropriate escape circuits to trigger backward walking, jumping and/or flying (Card and Dickinson, 2008; Sen et al., 2017; Tammero and Dickinson, 2002).

In *Drosophila melanogaster*, an equidistant long vertical object and a small object elicit visually evoked steering responses of opposite valence, implementing a simple object classification algorithm that enables flies to approach an elongated vertical bar, which likely represents a landscape feature (van Breugel and Dickinson, 2012), while avoiding a small object, which likely represents a threat or conspecific (Maimon et al., 2008). However, small-object aversion does not generalize across all *Drosophila* species, suggesting ecology-dependent specialization (Park and Wasserman, 2018). At present, the behavioral strategy in *D. melanogaster* that generates approach and aversion is unclear. The object classification system that distinguishes between tall and small objects must link visual information to an appropriate motor action to orient the animal toward or away from the stimulus (Maimon et al., 2008).

Previous work showed that tethered, flying flies that are free to rotate about the yaw axis perform body saccades toward a moving, tall vertical bar and the dynamics of these saccades can be predicted by integrating the angular position of the bar relative to the fly's forward axis over time. These results are consistent with a model in which the fly brain temporally integrates the angular position of the bar relative to its body axis over time, until this value reaches a threshold, to trigger (with noise) a saccade toward the bar (Mongeau and Frye, 2017). Such an underlying visuomotor algorithm, characterized in tethered flight, is one way to explain why flies in free flight aggregate near tall vertical objects. It remains unknown whether small-object aversion is also controlled by saccades and how saccades and smooth movement interact. Here, we hypothesized that small-object aversion relies on a distinct behavioral strategy that generates larger, visually guided saccades that could enable avoidance of a potential threat or conspecific. To test this hypothesis, we studied the behavioral strategy that underlies bar tracking and small-object aversion by studying flight in a rigid- and magnetic-tether paradigm. We discovered that aversion to a motion-defined object is mediated by saccades oriented away from the small object. Together, our results support the hypothesis that object classification and saccade-based behavioral algorithms for approach and avoidance are distinct.

MATERIALS AND METHODS

Animals

A wild-type *Drosophila melanogaster* Meigen 1830 strain was maintained at 25°C under a 12 h:12 h light:dark cycle with access to food and water *ad libitum*. This *D. melanogaster* strain was reared from a wild-caught iso-female line. All experiments were performed with 3–5 day old adult female flies.

Visual stimuli

Most tethered behavioral experiments in virtual reality flight simulators have historically used stimuli composed of solid dark objects or black-and-white gratings superimposed on a uniform white background (Gotz, 1968; Hassenstein and Reichardt, 1956). These visual objects, though convenient and intuitive, can be discriminated from the visual background by any combination of luminance, contrast or motion cues. These visual cues may drive motion vision and feature detection differently. Figures composed of random

Department of Integrative Biology and Physiology, University of California - Los Angeles, Los Angeles, CA 90095-7239, USA.
*Present address: Department of Mechanical Engineering, Pennsylvania State University, University Park, PA 16802, USA.

‡Author for correspondence (jmmongeau@psu.edu)

J.-M.M., 0000-0002-3292-6911; M.A.F., 0000-0003-3277-3094

Received 2 October 2018; Accepted 10 December 2018

texture superimposed upon a similarly random background are defined only by their motion relative to the background, yet nevertheless elicit robust figure–ground discrimination in flies rigidly tethered under virtual (experimentally coupled) closed-loop feedback conditions, even when the figure is defined by higher order statistical properties that are undetectable by a classical model of motion vision (Aptekar et al., 2012; Fox et al., 2014; Theobald et al., 2008). Furthermore, a motion-defined vertical bar elicits more robust saccadic tracking than a similarly sized dark bar against a uniform background (Mongeau and Frye, 2017). The different experimental approaches used here were designed to show: (1) saccadic steering responses (spikes in the change in wingbeat amplitude, ΔWBA) by a rigidly tethered fly in response to sinusoidal object movement centered at a fixed azimuthal location (Fig. 1C; Fig. S1); (2) saccade orientation and amplitude tuning by rigidly tethered flies in response to varying object size at all azimuthal locations (Fig. 1D,E); and (3) how saccade dynamics for object approach and avoidance map onto the behavior of flies operating in the more naturalistic magnetically tethered paradigm (Fig. 2).

Rigid-tether paradigm

After cold-anesthetizing flies, we glued a small tungsten pin onto the thorax using UV-activated glue. Flies were given at least 1 h to recover prior to experiments. Flies were then placed in the center of a cylindrical flight arena (Fig. 1A). The arena has been described elsewhere (Reiser and Dickinson, 2008). The display consisted of a cylindrical array of 96×32 LEDs subtending 330 deg horizontally and 94 deg vertically. An infrared diode was used to project light onto the beating wings, casting a shadow onto an optical sensor. A wingbeat analyzer (JFI Electronics, Chicago, IL, USA) transformed the signal from the optical sensor into a signal that is proportional to the WBA of the left wing minus that of the right wing. ΔWBA signals from the optical wingbeat analyzer were acquired at 1000 Hz.

As shown in Fig. 1C, each fly was presented with 6 s of open-loop virtual object motion followed by 5 s of closed-loop bar fixation. The open-loop stimulus motion was sinusoidal; specifically, the object oscillated at 1 Hz and moved 22.5 deg in each direction from its starting position at ±45 deg from visual midline (angular speed=90 deg s^{-1}). This 6 s stimulus epoch was repeated until each fly was presented with each bar height variation 12 times, resulting in approximately 4 min of stimulus per fly. The height of the tall and short bar was 94 and 15 deg, respectively, and width was kept constant at 30 deg. We show the averaged response for an object on the fly's right, in addition to several raw traces. A subset of the full dataset of raw trials is contained in Fig. S1. The motion-defined (Fourier) object was composed of vertical stripes with an equal number of ON and OFF columns superimposed over a background with the same statistics, i.e. equal number of ON and OFF columns.

To quantify how bar height affects torque spike valence and amplitude, we employed the Spatio-Temporal Active Field (STAF) methodology, as described previously (Aptekar et al., 2012, 2014). Briefly, the path of a bar of variable height was prescribed by a pseudo-random, 15.6 s m-sequence. Thus, the bar 'jittered' around a fixed azimuthal location and ΔWBA spikes were identified from the ΔWBA signal as described in prior work (Aptekar et al., 2012). The initial bar position was set at 24 equally spaced azimuthal positions; therefore, each fly went through 24 stimulus trials, one at each of 24 randomly shuffled azimuthal locations.

Magnetic tether paradigm

Animals were prepared for each experiment according to a protocol that has been described previously (Bender and Dickinson, 2006; Duistermars and Frye, 2008). Briefly, flies were cold anesthetized by cooling on a stage maintained at approximately 4°C. For the magnetic tether, stainless steel pins (100 µm diameter; Fine Science Tools, Foster City, CA, USA) were glued onto the thorax by applying UV-activated glue. The pins comprised less than 1% of the fly's moment of inertia about the yaw axis. Flies were allowed at least 1 h to recover before running experiments.

The magnetic tether system has been described elsewhere (Bender and Dickinson, 2006; Duistermars and Frye, 2008). Briefly, the display consisted of an array of 96×16 light emitting diodes (LEDs, each subtending 3.75 deg on the eye) that wrap around the fly, subtending 360 deg horizontally and 56 deg vertically (Fig. 2A). Flies were suspended between two magnets, allowing free rotation along the vertical (yaw) axis and illuminated from below with an array of eight 940 nm LEDs. The angular position of the fly within the arena was recorded at 160 frames s^{-1} with an infrared (IR)-sensitive camera placed directly below the fly (A602f, Basler, Ahrendburg, Germany).

After suspending the fly within the magnetic field, flies were given several minutes to acclimate. We began each experiment by eliciting sustained rotation of the fly by rotating a visual panorama either clockwise or counterclockwise for 30 s at 120 deg s^{-1}. This stimulus elicited a strong rotatory, yaw-based smooth co-directional optomotor turning response with occasional saccades. From these data, we estimated the fly's point of rotation by computing the cumulative sum of all camera frames and measuring its centroid. Flies that could not robustly follow the rotating panorama were not used in experiments.

To study the flies' responses to tall and short bars, we rotated a motion-defined, 8-pixel-wide (30 deg) bar on a randomly generated background of 'on' and 'off' pixels (Fig. 2B). The bar's initial azimuth position in the arena was generated from a pseudo-random sequence. We rotated the bar at 113 deg s^{-1} and randomized the direction of motion (clockwise/counterclockwise) and bar type (short and tall bar) to minimize habituation. We presented each stimulus for a period of 30 s, defining the duration of an individual trial. Between each trial, we presented a fixed visual landscape for 25 s for the fly to rest. If flies stopped flying during a trial, the trial was discarded. We ignored the first 1 s of a trial in order to avoid the inclusion of saccades that could be generated when the stimulus first appears. We rejected saccades below 10 deg and above 180 deg in amplitude in order to exclude possible tracking error. The procedure to identify saccades from heading data has been described elsewhere (Mongeau and Frye, 2017). Briefly, we modeled the fly as an ellipsoid and determined the heading by calculating the major axis of the ellipse in each video frame.

Statistical analysis

All statistical analysis was performed using Matlab (MathWorks, Natick, MA, USA) and JMP (SAS, Cary, NC, USA). Unless otherwise specified, we report mean±1 s.d. For box plots, the central line is the median, the bottom and top edges of the box are the 25th and 75th percentiles and the whiskers extend to ±2.7 s.d.

RESULTS AND DISCUSSION

To determine whether flies perform saccadic turns away from short visual objects, analogous to how they perform saccades to steer toward tall, narrow objects, we measured the steering effort of flies in response to oscillating bar motion in tethered flight. A randomly textured motion-defined tall bar or a short bar was presented at ±45 deg from the center of the arena (0 deg). The bar oscillated at 1 Hz and moved 22.5 deg in each direction from its starting position at

Journal of Experimental Biology (2019) 222, jeb193730. doi:10.1242/jeb.193730

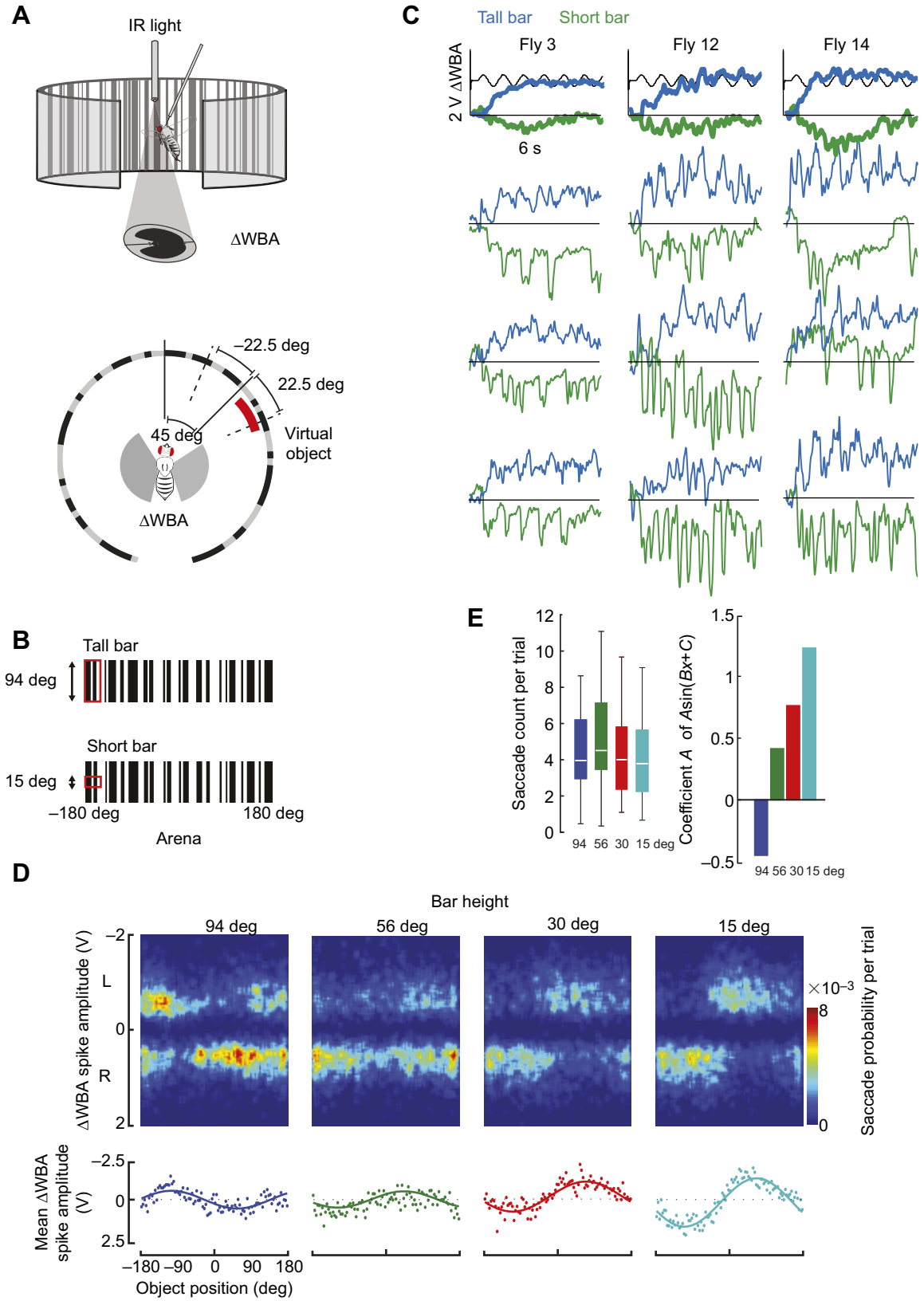

Fig. 1. See next page for legend.

Journal of Experimental Biology (2019) 222, jeb193730. doi:10.1242/jeb.193730

Fig. 1. Bar height influences saccade valence in open-loop tethered flight in a rigid tether. (A) Flies were rigidly tethered and their steering response – changes in wingbeat amplitude (ΔWBA) – measured by an optical wingbeat analyzer. Flies were illuminated with infrared (IR) light. A moving virtual object was presented at ±45 deg from the center of the arena (0 deg). The object oscillated at 1 Hz and moved 22.5 deg in each direction from its starting position at ±45 deg. (B) Top: tall bar stimulus with height=94 deg, spanning the full height of the display. Bottom: short bar stimulus with height=15 deg. Stimulus width=30 deg. (C) Top: average fly steering ΔWBA responses for n=3 flies in response to tall and short objects displaced to the right of the fly. For the tall bar, the steering response is tonically oriented towards the position of the bar. For the short bar, the steering offset is oriented away from the bar position. Bottom panels: three exemplar individual trials showing ΔWBA spikes. Subset of dataset from n=18 flies is in Fig. S1. (D) Top: surface histograms mapping ΔWBA spike amplitude (pseudocolor) oriented toward the left or right (vertical axis) for 24 different bar locations (horizontal axis) and different virtual object height. Bottom: average saccade amplitude at each azimuthal location with sinusoidal fits by azimuthal position (same data as in top). Bar width was kept constant at 30 deg, and bar height was varied between 94 deg (tall bar – full height of arena), 56 deg, 30 deg and 15 deg (short bar). (E) Saccade count per trial (left) and best-fit amplitude coefficient of sinusoid in D for different object heights. n=30 flies, 24 trials per fly, for D and E.

±45 deg (Fig. 1A,B). Confirming the results of a previous study that used solid black bars on a uniform background (Maimon et al., 2008), on average flies steered toward a tall textured bar and avoided a short bar moving across a static random background (Fig. 1C). Averaging across trials masks the dynamics of the behavior for fixation and aversion. The spikes in ΔWBA – which have been referred to as 'wing hitches' (Heide and Götz, 1996) or 'torque spikes' by direct torque measurements in tethered flight (Heisenberg and Wolf, 1979) – indicate attempted body saccades. ΔWBA spikes were readily observed within single trials that were generally oriented toward the tall bar and away from the short bar located 45 deg from the visual midline (Fig. 1C; Fig. S1). ΔWBA spikes were superimposed upon a shift in mean ΔWBA toward the tall bar and away from the short bar (Fig. 1C; Fig. S1), consistent with prior work (Maimon et al., 2008).

The raw traces from multiple flies (Fig. 1C) would seem to suggest not only that the valence of ΔWBA spikes switches with bar size but also that the short bar might elicit ΔWBA spikes with distinct dynamics. To explore the distribution of saccadic steering spikes across the full visual azimuth, and how saccade dynamics vary with object size, we used an experimental method in which a bar was randomly jittered at each of 24 azimuthal positions (Aptekar et al., 2012, 2014). We randomly shuffled trials for bar vertical heights of 94 deg (tall bar, full height of arena), 56 deg, 30 deg and 15 deg (short bar). We measured the amplitude of individual ΔWBA spikes binned at 24 azimuthal position (Fig. 1D). This analysis revealed a switch of sign and increased amplitude in ΔWBA spikes as the bar height decreased (Fig. 1D,E). The overall ΔWBA spike rate was similar across object height (Fig. 1E). However, the ΔWBA spike amplitude in the rigid tether must be interpreted with caution as different tonic ΔWBA levels between short and tall bars could bias ΔWBA spike amplitude.

To test whether body saccades drive short bar aversion under more naturalistic feedback conditions, we recorded flight responses in a magnetic tether system (Bender and Dickinson, 2006; Duistermars and Frye, 2008). This experimental paradigm allowed flies to freely rotate in yaw, thereby enabling more naturalistic flight dynamics and neural feedback conditions (Fig. 2A). As in the rigid tether system, we presented an object rotating over a randomly textured stationary background. We confirmed that a rotating tall bar elicited robust, attractive tracking saccades, i.e. saccades that bring the bar closer to visual midline (Mongeau and Frye, 2017). We discovered that a rotating short bar elicited more aversive saccades, i.e. saccades that move the bar further away from visual midline (Fig. 2B,C). Together, these results suggest that bar height has a strong effect on saccade valence, supporting results in the rigid-tether paradigm.

Notably, there was little-to-no smooth pursuit between saccades during the presentation of a small motion-defined bar (Fig. 2E). To reconcile the lack of smooth movement in the magnetic tether with previous studies in a rigid-tether paradigm using a dark bar on a uniform background that showed strong tonic steering responses (Maimon et al., 2008), we performed an experiment using the magnetic tether where we revolved a motion-defined or dark bar at constant speed (75 deg s^{-1}). We found that the short dark bar generated robust smooth movement between saccades whereas a short motion-defined bar revolving at the same speed generated little-to-no smooth movement (Fig. 2E). The smooth movement in response to a short, dark bar in the magnetic tether is co-directional, which is consistent with the in-phase oscillations when a small object oscillates at the fly's visual midline in the rigid tether (Maimon et al., 2008). Therefore, flies can use saccades to perform orienting behavior, but they can also generate slower smooth pursuit, which varies with the stimulus type (Keleş et al., 2018).

In some cases, short bars elicited bouts of co-directional saccades seemingly being chased by the object, whereas in other cases flies generated bouts of contra-directional saccades away from the object (Fig. 2B). To clarify whether flies generally saccade to avoid the small bar, we defined tracking saccades as sustained, co-directional saccades in the same direction as the bar for at least 180 deg around the arena (bout of 4–5 saccades), following a previous study (Mongeau and Frye, 2017). Using this operational definition, flies overall generated 36% tracking saccades in the presence of a tall bar (fly following bar) and 2% in the presence of a short bar (fly chased by bar), thus suggesting more robust, sustained tracking in the presence of a tall bar (Fig. 2D).

A higher median rate of saccades was generated for the tall bar than for the short bar (tall bar: 1.1 saccades s^{-1}, short bar: 0.63 saccades s^{-1}). The short bar saccade rate was higher than previously reported spontaneous saccade rates in the magnetic tether (~0.4 saccades s^{-1}) (Bender and Dickinson, 2006; Mongeau and Frye, 2017), suggesting that the short bar stimulus elicited visually guided saccades. However, we expect that some saccades we measured were spontaneous, triggered by endogenous processes (Ferris et al., 2018; Schnell et al., 2017). Nevertheless, there was a significant association between the stimulus type and saccade valence (χ^2 test, P<0.001, d.f.=1, n=2833 saccades). For the short bar, there were more aversive saccades than predicted by chance (χ^2 test, P=0.001, d.f.=1, n=877 saccades), whereas for the tall bar, there were more attractive saccades than predicted by chance (χ^2 test, P<0.001, d.f.=1, n=1956 saccades). The amplitude, duration and peak angular velocity of saccades in the magnetic tether were overall smaller for the tall bar than for the short bar (t-test, P<0.001, d.f.=1, n=2833 saccades; Fig. 2F), which is consistent with the findings in the rigid tether (Fig. 1D). The statistical outcome did not change when considering non-parametric distributions (Kruskal–Wallis test) or the possible effect of individuals (mixed-effect model). To determine whether the pre-saccade error angle could be influencing the saccade dynamics, we computed the pre-saccade error angle in azimuth for both tall- and short-bar experiments. For the tall bar, the pre-saccade error angle was centered at ~45–60 deg and correlated with saccade amplitude, consistent with our previous work (Fig. 2G) (Mongeau and Frye, 2017). In contrast, for a motion-defined short bar, the pre-saccade error angle was more stochastic, with a wider distribution (Fig. 2G), and findings were similar for a short, dark bar (Fig. S2). These data

Journal of Experimental Biology (2019) 222, jeb193730. doi:10.1242/jeb.193730

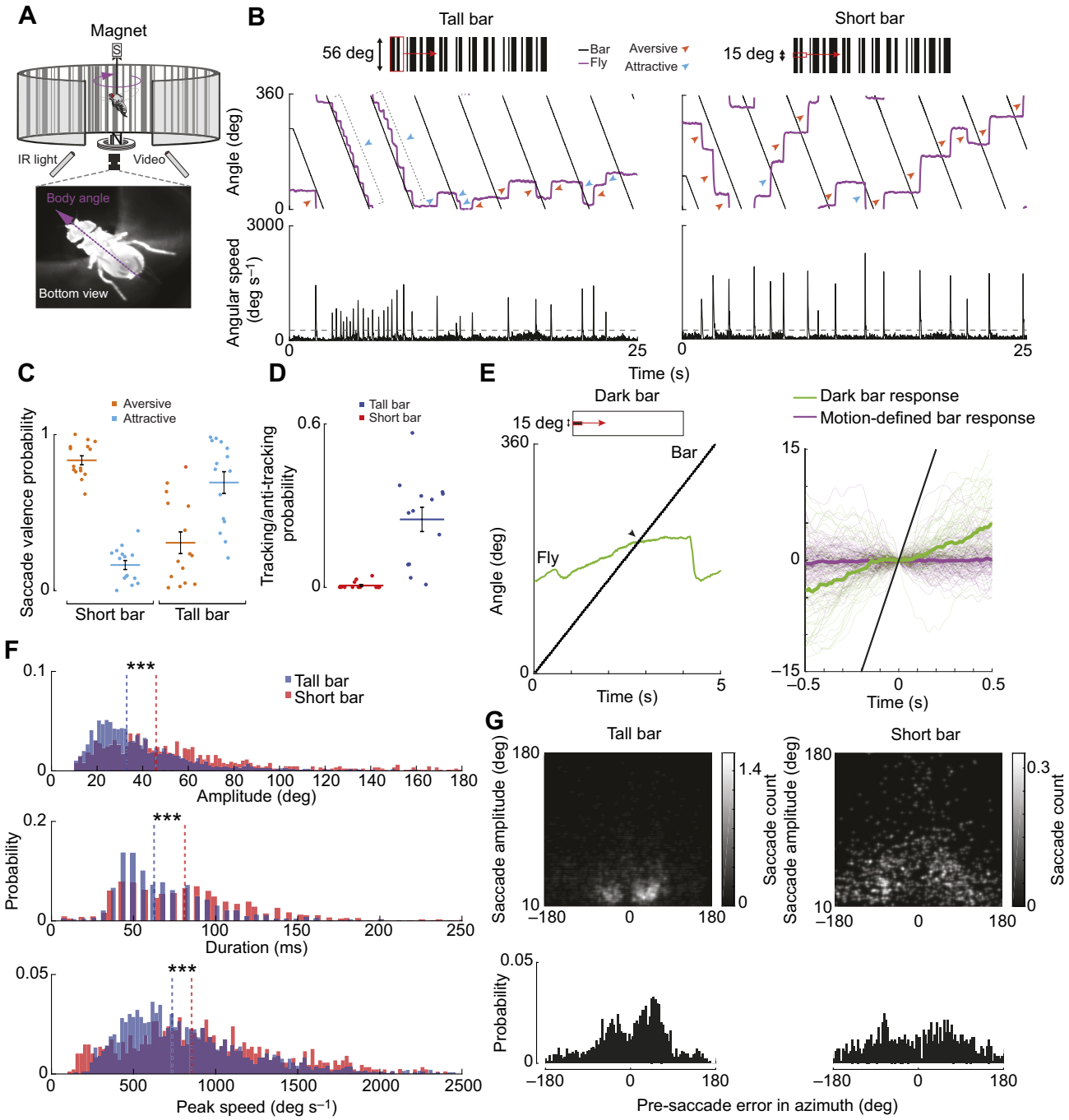

Fig. 2. Bar height influences saccade tuning in a magnetic tether. (A) Flies were suspended magnetically and free to rotate about the yaw axis. We used high-speed video (160 frames s^{-1}) and offline image processing to track the fly's body angle. Flies were illuminated with IR light. (B) Left: a fly fixates a moving tall bar (56 deg height, full vertical height of arena) by generating bouts of attractive saccades and some aversive saccades. Right: flies generate a primarily aversive saccade in response to a moving short bar (15 deg height). Virtual object width=30 deg. Bottom: angular speed of fly body angle. Gray dotted line: computed saccade detection threshold. Bar speed: 113 deg s^{-1}. (C) Distribution of saccade valence probability during the presentation of a tall and short bar. Thick line: mean. Error bar: s.e.m. Individual dots are the mean for an individual fly. (D) Probability of flies generating bouts of tracking saccades via sustained, co-directional saccades covering 180 deg of the arena. Thick line: mean. Error bar: s.e.m. Individual dots are the mean for an individual fly. (E) Left: example response to motion of a small, dark bar via smooth movement and saccades. Arrow indicates midline crossing. Right: comparison of inter-saccade body angles during the presentation of short, motion-defined (red) and dark (green) bars. t=0 s is the fly's visual midline. Thick line: median. Stimulus: black line. Stimulus speed=75 deg s^{-1}. n=5 flies, 80 trials. (F) Histograms of saccade amplitude, duration and peak angular speed for a tall bar (blue) and a short bar (red). ***$P \leq 0.001$. Dashed lines: median. (G) Top: colormap of pre-saccade error in azimuth versus saccade amplitude for motion-defined tall and short bars. 0 deg is the fly's visual midline. Bottom: probability histogram of pre-saccade error angles. For C,D,F,G: n=14 animals, 150 trials total.

show that the error angles that generate saccades have substantially different distributions between a tall and short bar, suggesting different trigger algorithms. The difference in saccade dynamics and trigger suggest that saccades are highly adaptable, as discovered in avoidance and spontaneous saccades in free flight (Muijres et al., 2014, 2015).

Together, the behavioral responses measured in the rigid and magnetic tether to the presentation of a tall bar and a short bar

suggest that the approach and aversion flight orientation responses in *D. melanogaster* are driven by processes that elicit signed saccades with distinct dynamics (Figs 1D,E and 2). Prior work had revealed a simple visual algorithm by which the vertical size of an object controls a switch from visual approach to aversion (Maimon et al., 2008). The evidence for the size-dependent valence switch, which we confirm here, was that under open-loop tethered-flight conditions, steering responses to an object oscillating in the visual periphery were tonically oriented toward an elongated bar and away from a small object, with phasic modulations in steering that track the sinusoidal oscillation of the stimulus (Fig. 1C). Likewise, flies fixate a tall vertical bar but avoid a short bar in closed-loop tethered flight (Maimon et al., 2008). Our results go substantially further by demonstrating that: (1) small-object classification by the visual system outputs saccades as well as smooth movement, which depends on the stimulus type; (2) a small object triggers more aversive saccades (Figs 1D,E and 2C); and (3) small-object aversion saccades have significantly different dynamics and trigger mechanisms from bar-tracking saccades (Fig. 2F,G). Thus, as with bar tracking (Mongeau and Frye, 2017), small-object aversion behavior in flight is mediated in part by body saccades. Our study provides new hypotheses to interrogate the neural basis of object classification for decision making in insects.

Acknowledgements
We thank Nadya Zolotova for data collection.

Competing interests
The authors declare no competing or financial interests.

Author contributions
Conceptualization: J.-M.M., J.A., M.A.F.; Methodology: J.-M.M., J.A., M.A.F.; Formal analysis: J.-M.M., K.Y.C., J.A.; Investigation: J.-M.M., K.Y.C., J.A.; Writing - original draft: J.-M.M., M.A.F.; Writing - review & editing: J.-M.M., M.A.F.; Supervision: M.A.F.; Project administration: M.A.F.; Funding acquisition: M.A.F.

Funding
This work was funded by the National Institutes of Health R01EY026031 (M.A.F.). Deposited in PMC for release after 12 months.

Supplementary information
Supplementary information available online at
http://jeb.biologists.org/lookup/doi/10.1242/jeb.193730.supplemental

References
Aptekar, J. W., Shoemaker, P. A. and Frye, M. A. (2012). Figure tracking by flies is supported by parallel visual streams. *Curr. Biol.* **22**, 482-487.

Aptekar, J. W., Keles, M. F., Mongeau, J.-M., Lu, P. M., Frye, M. A. and Shoemaker, P. A. (2014). Method and software for using m-sequences to characterize parallel components of higher-order visual tracking behavior in Drosophila. *Front. Neural Circuits* **8**, 130.

Bender, J. A. and Dickinson, M. H. (2006). Visual stimulation of saccades in magnetically tethered Drosophila. *J. Exp. Biol.* **209**, 3170-3182.

Card, G. and Dickinson, M. H. (2008). Visually mediated motor planning in the escape response of Drosophila. *Curr. Biol.* **18**, 1300-1307.

Duistermars, B. J. and Frye, M. (2008). A magnetic tether system to investigate visual and olfactory mediated flight control in Drosophila. *J. Vis. Exp.* e1063.

Ferris, B. D., Green, J. and Maimon, G. (2018). Abolishment of spontaneous flight turns in visually responsive Drosophila. *Curr. Biol.* **28**, 170-180.e5.

Fox, J. L., Aptekar, J. W., Zolotova, N. M., Shoemaker, P. A. and Frye, M. A. (2014). Figure-ground discrimination behavior in Drosophila. I. Spatial organization of wing-steering responses. *J. Exp. Biol.* **217**, 558-569.

Frye, M. A. and Dickinson, M. H. (2001). Fly flight: a model for the neural control of complex behavior. *Neuron* **32**, 385-388.

Gotz, K. G. (1968). Flight control in Drosophila by visual perception of motion. *Kybernetik* **4**, 199-208.

Hassenstein, B. and Reichardt, W. (1956). Systemtheoretische Analyse der Zeit-, Reihenfolgen- und Vorzeichenauswertung bei der Bewegungsperzeption des Rüsselkäfers Chlorophanus. *Z. Naturforsch. B* **11**, 513-524.

Heide, G. and Götz, K. G. (1996). Optomotor control of course and altitude in Drosophila melanogaster is correlated with distinct activities of at least three pairs of flight steering muscles. *J. Exp. Biol.* **199**, 1711-1726.

Heisenberg, M. and Wolf, R. (1979). On the fine structure of yaw torque in visual flight orientation of Drosophila melanogaster. *J. Comp. Physiol. A* **130**, 113-130.

Keleş, M. F., Mongeau, J.-M. and Frye, M. A. (2018). Object features and T4/T5 motion detectors modulate the dynamics of bar tracking by Drosophila. *J. Exp. Biol.* **221**, jeb.190017.

Maimon, G., Straw, A. D. and Dickinson, M. H. (2008). A simple vision-based algorithm for decision making in flying Drosophila. *Curr. Biol.* **18**, 464-470.

Mongeau, J.-M. and Frye, M. A. (2017). Drosophila spatiotemporally integrates visual signals to control saccades. *Curr. Biol.* **27**, 2901-2914.e2.

Mongeau, J.-M., Sponberg, S. N., Miller, J. P. and Full, R. J. (2015). Sensory processing within cockroach antenna enables rapid implementation of feedback control for high-speed running maneuvers. *J. Exp. Biol.* **218**, 2344-2354.

Muijres, F. T., Elzinga, M. J., Melis, J. M. and Dickinson, M. H. (2014). Flies evade looming targets by executing rapid visually directed banked turns. *Science* **344**, 172-177.

Muijres, F. T., Elzinga, M. J., Iwasaki, N. A. and Dickinson, M. H. (2015). Body saccades of Drosophila consist of stereotyped banked turns. *J. Exp. Biol.* **218**, 864-875.

Park, E. J. and Wasserman, S. M. (2018). Diversity of visuomotor reflexes in two Drosophila species. *Curr. Biol.* **28**, R865-R866.

Reiser, M. B. and Dickinson, M. H. (2008). A modular display system for insect behavioral neuroscience. *J. Neurosci. Methods* **167**, 127-139.

Schnell, B., Ros, I. G. and Dickinson, M. H. (2017). A descending neuron correlated with the rapid steering maneuvers of flying Drosophila. *Curr. Biol.* **27**, 1200-1205.

Sen, R., Wu, M., Branson, K., Robie, A., Rubin, G. M. and Dickson, B. J. (2017). Moonwalker descending neurons mediate visually evoked retreat in Drosophila. *Curr. Biol.* **27**, 766-771.

Tammero, L. F. and Dickinson, M. H. (2002). Collision-avoidance and landing responses are mediated by separate pathways in the fruit fly, Drosophila melanogaster. *J. Exp. Biol.* **205**, 2785-2798.

Theobald, J. C., Duistermars, B. J., Ringach, D. L. and Frye, M. A. (2008). Flies see second-order motion. *Curr. Biol.* **18**, R464-R465.

van Breugel, F. and Dickinson, M. H. (2012). The visual control of landing and obstacle avoidance in the fruit fly Drosophila melanogaster. *J. Exp. Biol.* **215**, 1783-1798.

Wu, M., Nern, A., Williamson, W. R., Morimoto, M. M., Reiser, M. B., Card, G. M. and Rubin, G. M. (2016). Visual projection neurons in the Drosophila lobula link feature detection to distinct behavioral programs. *eLife* **5**, e21022.